Function of Glu-469′ in the Acid−Base Catalysis of Thioredoxin Reductase from *Drosophila melanogaster*[†]

Hsin-Hung Huang, L. David Arscott, David P. Ballou, and Charles H. Williams, Jr.*

Department of Biological Chemistry, University of Michigan Medical School, Ann Arbor, Michigan 48109-0606

Received August 1, 2008; Revised Manuscript Received October 7, 2008

ABSTRACT: Thioredoxin reductase (TrxR) catalyzes the reduction of thioredoxin (Trx) by NADPH. Because dipteran insects such as *Drosophila melanogaster* lack glutathione reductase, their TrxRs are particularly important for antioxidant protection; reduced Trx reacts nonenzymatically with oxidized glutathione to maintain a high glutathione/glutathione disulfide ratio. Like other members of the pyridine nucleotide-disulfide oxidoreductase family, TrxR is a homodimer; in the enzyme from *D. melanogaster* (DmTrxR), each catalytically active unit consists of three redox centers: FAD and an N-terminal Cys-57−Cys-62 redox-active disulfide from one monomer and a Cys-489′−Cys-490′ C-terminal redox-active disulfide from the second monomer. A dyad of His-464′ and Glu-469′ in TrxR acts as the acid−base catalyst of the dithiol−disulfide interchange reactions required in catalysis [Huang, H.-H., et al. (2008) *Biochemistry 47*, 1721−1731]. In this investigation, the role of Glu-469′ in catalysis by DmTrxR has been studied. The E469′A and E469′Q DmTrxR variants retain 28 and 35% of the wild-type activity, respectively, indicating that this glutamate residue is important but not critical to catalysis. The pH dependence of V_{max} for both glutamate variants yields pK_a values of 6.0 and 8.7, compared to those in the wild-type enzyme of 6.4 and 9.3, respectively, indicating that the basicity of His-464′ in TrxR in complex with its substrate, DmTrx-2, is significantly lower in the glutamate variants than in wild-type enzyme. The rates of some steps in the reductive half-reactions in both glutamate variants are much slower than those of the wild-type enzyme. On the basis of our observations, it is proposed that the function of Glu-469′ is to facilitate the positioning of His-464′ toward the interchange thiol, Cys-57, as suggested for the analogous residue in glutathione reductase.

Thioredoxin reductase (TrxR,[1] EC 1.6.4.5) is a member of the pyridine nucleotide-disulfide oxidoreductase family that includes glutathione reductase, lipoamide dehydrogenase, trypanothione reductase, peroxiredoxin reductase, and mercuric reductase (*1, 2*). The enzyme catalyzes the reaction $NADPH + H^+ + Trx(S)_2 \leftrightarrows NADP^+ + Trx(SH)_2$ (*3*). The Trx system mediates a wide variety of physiological functions in cells, and an excellent summary of its roles in eukaryotes has appeared recently (*4, 5*).

The Trx system has been shown to be crucial in dipteran insects such as *Drosophila melanogaster* and *Anopheles gambiae*, the major vector of tropical malaria, because glutathione reductase is absent in these organisms (*6*). Reduced Trx is able to reduce glutathione disulfide (GSSG) nonenzymatically to maintain a high ratio of GSH to GSSG, which is important for defense against reactive oxygen species. TrxRs from *D. melanogaster* and *A. gambiae* are closely related (69% identical), and the residues that contribute to the active sites of the two enzymes are virtually identical (*7, 8*). Thus, TrxR from *D. melanogaster* (DmTrxR), for which a crystal structure is available (*9*), offers an excellent model for TrxRs from dipteran insects.

DmTrxR is a high-M_r TrxR with a monomer molecular mass of ~55000 Da. Like other high-M_r TrxRs, DmTrxR is a dimeric flavoprotein (*8, 10, 11*). The mechanistically active groups in DmTrxR consist of three redox centers: FAD, an N-terminal disulfide (Cys-57−Cys-62) that is adjacent to the flavin from one subunit, and a second disulfide (Cys-489′−Cys-490′) that is penultimate to the C-terminal serine residue from the other subunit (*9*). A catalytic mechanism of DmTrxR has been proposed (*8, 11, 12*) as shown in Scheme 1; however, for the sake of clarity, some of the protonation−deprotonation steps are not explicitly included. In step k_1, NADPH is bound to the *re* side of the isoalloxazine ring of FAD, and in step k_3, a hydride ion is passed from NADPH to reduce FAD, forming a $FADH^-$−$NADP^+$ charge-transfer complex (CTC) (EH_2^A in Scheme 1). The reducing equivalents are then passed from $FADH^-$ to the N-terminal redox-active disulfide (Cys-57−Cys-62), which is adjacent to the *si* side of the isoalloxazine ring of FAD, and a CTC of thiolate (Cys-62) to FAD is formed (EH_2^B in Scheme 1). Subsequently, reducing equivalents are passed from the nascent N-terminal dithiol to the C-terminal redox-

[†] This work was supported by grants from the National Institute of General Medical Sciences (GM11106).

* To whom correspondence should be addressed: Department of Biological Chemistry, University of Michigan Medical School, Ann Arbor, MI 48109-0606. E-mail: chaswill@umich.edu. Phone: (734) 647-6989. Fax: (734) 763-4581.

[1] Abbreviations: CTC, charge-transfer complex (donor−acceptor); DmTrxR, thioredoxin reductase from *Drosophila melanogaster*; EH_2, two-electron-reduced enzyme; EH_4, four-electron reduced enzyme; FAD, flavin adenine dinucleotide; GSH, glutathione; GSSG, glutathione disulfide; LBHB, low-barrier hydrogen bond; PfTrxR, thioredoxin reductase from *Plasmodium falciparum*; Trx, thioredoxin; TrxR, thioredoxin reductase.

10.1021/bi801449h CCC: $40.75
Published on Web 11/08/2008

Scheme 1: Proposed Catalytic Mechanism of Wild-Type DmTrxR[a]

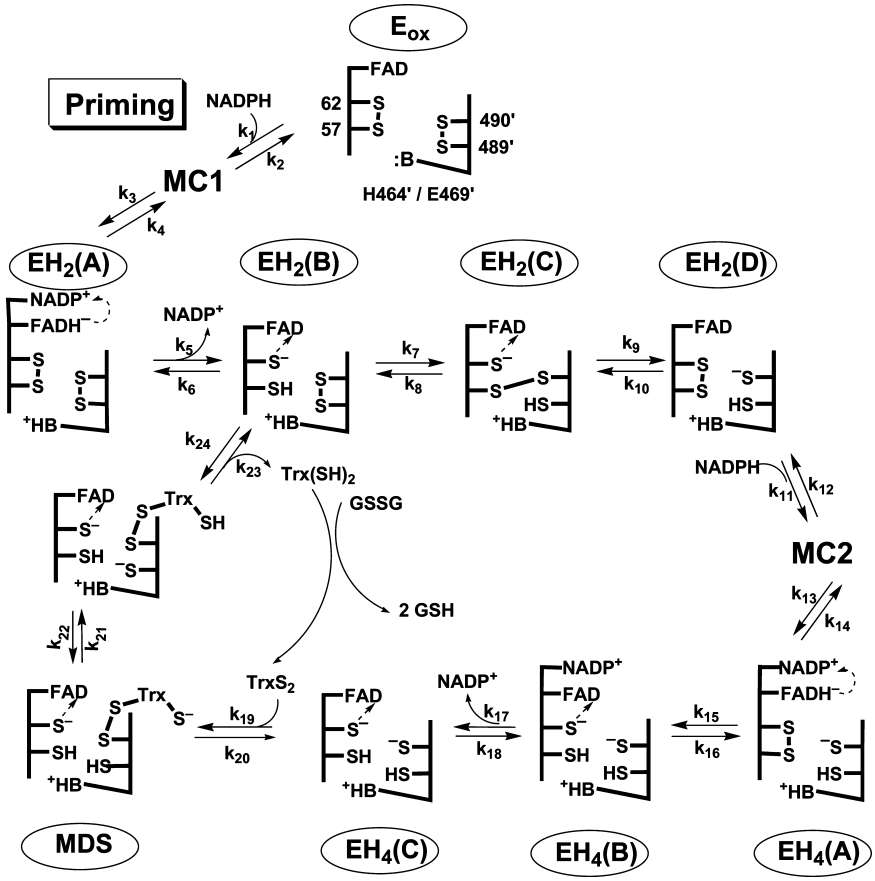

[a] The reductive half-reaction involves the steps denoted by rate constants, k_1-k_{18}, and the oxidative half-reaction involves steps $k_{19}-k_{24}$. MC, Michaelis complex; MDS, mixed disulfide. Charge transfer is indicated by a dashed arrow. Residues numbered without a prime come from one monomer, and those with a prime come from the other monomer. While there is no direct evidence to show that Cys-490′ is the nucleophile that attacks the disulfide bond of DmTrx, Cys-490′ in DmTrxR occupies the same position as Sec-489′ in mammalian TrxR. Because Sec-489′ is believed to undergo nucleophilic attack on Trx, Cys-490′ in DmTrxR is thought to be a nucleophile to attack the disulfide bond of DmTrx. Data in Bauer et al. indicate that the S of Cys-490′ is attacked by Cys-57 in step k_7 and that the thiol of Cys-490′ initiates the dithiol−disulfide interchange with Trx (*8*).

active disulfide, in a dithiol−disulfide interchange reaction. Finally, the nascent C-terminal dithiol reduces thioredoxin (Trx). It has been shown that DmTrxR cycles between EH_2 and EH_4 in catalysis as shown in Scheme 1 (*8, 11*).

As the catalytic mechanism of DmTrxR implies, a thiolate anion on Cys-57 is required to initiate the dithiol−disulfide interchange reaction. A histidine residue has been shown to be important in the catalysis of TrxR (*13*). This histidine residue is able to act as a base catalyst to facilitate the formation of thiolate anion on Cys-57 and to stabilize the thiolate by the formation of an ion pair with the imidazolium of His-464′. A glutamate residue, Glu-469′, juxtaposed with the histidine residue has been suggested to be involved in the catalysis of TrxRs from humans and *Plasmodium falciparum* (*13*−*15*), but the actual function of this residue has not been clarified.

A similar dyad acting as a general acid−base catalyst has been identified in a variety of enzymes (*16, 17*). The functions of a triad in serine proteases have been studied extensively (*18*−*20*). Ser-195, His-57, and Asp-102 form a catalytic triad in chymotrypsin, and initially, Asp-102 was thought to be involved in a charge-relay system with His-57 to convert a weakly nucleophilic CH_2OH group on Ser-195 into a more reactive alkoxide ion, CH_2O^-. Recently, the charge-relay mechanism has been considered to be unlikely because the pK_a value of His-57 is greater than that of Asp-102 (*19*). Thus, Asp-102 would not be expected to be able to sequester a proton from His-57. Subsequent NMR studies suggest that a low-barrier hydrogen bond (LBHB, or short, very strong hydrogen bond) is involved in the catalysis. In chymotrypsin, His-57 and Asp-102 form a weak hydrogen bond in the ground state. However, during catalysis, a LHBH forms when the pK_a values of His-57 and Asp-102 closely match and the distance between these two amino acid residues becomes shorter than the sum of the van der Waals radii (i.e., the distance between the oxygen and nitrogen must be less than 2.65 Å). Formation of a LBHB is more favorable in a hydrophobic environment, and its formation is thought to lower the activation barrier of a reaction. However, the existence of the LBHB mechanism for chymotrypsin is contentious; the only support for this mechanism comes from results of a NMR study and a low deuterium fractionation factor of the hydrogen in the putative LBHB (*16, 21*).

The structure of glutathione reductase, a member of the same family of enzymes as TrxR, reveals that the distance between the glutamate oxygen and the histidine nitrogen in the dyad is only slightly longer than that associated with

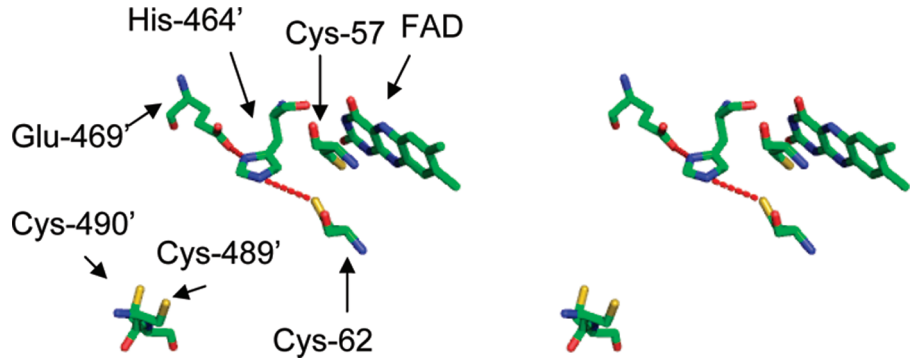

FIGURE 1: Stereoview showing the relative positions of the amino acid residues in the active site of DmTrxR. The active site contains a FAD, an N-terminal redox-active disulfide (Cys-57 and Cys-62), and a C-terminal redox-active disulfide (Cys-489′ and Cys-490′); the Ser-Cys-Cys-Ser motif is at the end of a flexible sequence of amino acid residues that could position Cys-489′ or Cys-490′ near the nascent N-terminal dithiol for the interchange reaction or alternately near the Trx binding site, as shown. His-464′ is adjacent to the N-terminal redox-active disulfide, and the distance between NE2 of His-464′ and the sulfur atom of Cys-57 is equal to 3.69 Å. The distance between ND1 of His-464′ and OE2 of Glu-469′ is 2.8 Å (*9*). PyMol was applied to generate the image, and the structure used here is based on the structure of rat TrxR (PDB entry 1H6V) (*33*).

LBHBs (2.8 Å) (*22, 23*). The role of the analogous glutamate-histidine dyad has been studied in another dithiol−disulfide dehydrogenase, lipoamide dehydrogenase, where the glutamate residue has been found to be able to modify the acid−base properties of the histidine residue. The glutamate residue is also likely to facilitate the orientation of the histidine residue toward the redox-active disulfide to make it more effective. Furthermore, the mutations that substitute glutamine and aspartate residues for glutamate change the electron distribution between the FAD and the redox-active cysteine pair (*24, 25*). The glutamate-histidine dyad juxtaposed with the N-terminal redox-active disulfide is conserved throughout the enzyme family that includes TrxR, and indeed, the glutamate variants of TrxR from *P. falciparum* and humans have been shown to have low activity (*13*−*15*). The function of this glutamate residue in the catalytic mechanism of TrxR has not been studied in detail despite the previously published data indicating its involvement in catalysis. On the basis of the crystal structure of DmTrxR (*9*), the distance between ND1 of His-464′ and OE2 of Glu-469′ is 2.8 Å, as shown in Figure 1. The structure of DmTrxR in the Protein Data Bank (PDB) is a monomer; however, the active site of DmTrxR is composed of residues from two subunits. Therefore, the structure of rat TrxR, which is highly related to DmTrxR, was used to illustrate the active site of DmTrxR. In addition, the glutamate and histidine residues are presumably in a hydrophobic environment. Thus, in analogy to chymotrypsin, it may be possible that a LBHB forms between His-464′ and Glu-469′ during catalysis, enabling this dyad to facilitate formation of thiolate anion on Cys-57.

To address the function of the glutamate residue in DmTrxR, we have studied the pH dependence of the steady-state kinetics of two glutamate variants, E469′Q and E469′A DmTrxRs, and the effect of pH on the properties of the glutamate variants undergoing the reductive half-reaction, including the rates of the three phases and the spectra of the intermediates.

MATERIALS AND METHODS

Chemicals. NADPH, lysozyme, FAD, phenylmethanesulfonyl fluoride, leupeptin, pepstatin, tricine, boric acid, citric acid, and GSSG were purchased from Sigma-Aldrich. Nickel-nitrilotriacetic acid agarose for purification of His-tagged proteins was from QIAGEN. Isopropyl β-D-thiogalactopyranoside was from Invitrogen. SDS−PAGE gels (4 to 20%) were purchased from NuSep. All other chemicals and reagents were from Fisher Scientific unless stated otherwise.

Site-Directed Mutagenesis. The plasmids of wild-type DmTrxR and DmTrx-2 were kindly provided by S. Gromer (University of Heidelberg, Heidelberg, Germany). The cDNA fragments encoding the genes of interest were inserted into the pQE-30 plasmid that allows expression of N-terminally His-tagged proteins. pQE-30 was obtained from QIAGEN. The sequence of each plasmid was verified by the sequencing core facility at the University of Michigan.

The cloning of the glutamate variants was performed using the QuikChange site-directed mutagenesis kit from Stratagene. The procedure in the manual provided by the manufacturer was followed. A plasmid, pQE-30, having the cDNA fragment of wild-type DmTrxR was used as a template to clone E469′A, E469′Q, and E470′A DmTrxRs. Another plasmid, pQE-30, containing the cDNA fragment of E469′A DmTrxR derived from the pervious experiment was applied as a template to clone E469′A/E470′A DmTrxR. The sequences of oligonucleotides used in this study are listed in Table S1 of the Supporting Information.

Preparation of the Glutamate Variants and the Substrate DmTrx-2. The methods were described previously (*12*). Briefly, the bacterial strain, NovaBlue from Novagen, was used for protein expression with induction by isopropyl β-D-thiogalactopyranoside. The harvested cells were suspended in buffer containing 50 mM potassium phosphate, 300 mM NaCl, and 10 mM imidazole. In the preparation of enzymes, 100 μM FAD was added to the lysate solution to stabilize the enzyme, and the bacteria were treated with lysozyme. The protease inhibitors, phenylmethanesulfonyl fluoride, leupeptin, and pepstatin, were added to cell lysates, and the lysates were sonicated. The six-His-tagged proteins were isolated from a nickel-nitrilotriacetic acid column with a step gradient of imidazole. All elution buffers for the preparation of enzymes contained 100 μM FAD. The procedures for isolation of enzymes and substrate were performed in the cold room (4 °C). The purity of each fraction of the glutamate variants and of DmTrx-2 was determined by analysis on 4

to 20% SDS−PAGE gel. The imidazole in each fraction was removed with a 10-DG desalting column from Bio-Rad. This procedure, which was quicker than dialysis, avoided the known instability of these proteins during dialysis. The concentrations of the DmTrxR glutamate variants and of DmTrx-2, the physiological substrate, were determined spectrally using an ε_{462} value of 11900 M^{-1} cm^{-1} for the enzyme and an ε_{277} value of 7320 M^{-1} cm^{-1} for the substrate (*8, 26*).

Determination of Activities of the Glutamate Variants. The activities were determined by the rates of consumption of NADPH, monitored at 340 nm in the presence of 100 μM NADPH, 50 μM DmTrx-2, and 0.3 mM GSSG in a universal buffer (pH 7.6) (*27*) containing 25 mM borate, 25 mM monobasic potassium phosphate, 25 mM tricine, and 25 mM citrate; this buffer does not maintain a constant ionic strength as the pH is changed. Results were corrected for the acid-catalyzed hydrolysis of NADPH.

Steady-State Kinetics of the Glutamine Variants over a Range of pH Values. The reaction rates of E469′A, E469′Q, and E469′A/E470′A DmTrxRs were determined at various pH values in the universal buffer by measuring the rate of consumption of NADPH using various concentrations of DmTrx-2 and a fixed concentration of NADPH (100 μM) in the presence of GSSG (0.3 mM); because the K_m of NADPH for the wild-type enzyme is less than 2 μM, it is not possible to determine the K_m value of NADPH accurately without resorting to fluorescence techniques (*12*). K_m and V_{max} values were derived from a Michaelis−Menten graph of turnover number versus concentration of DmTrx-2 fit by the equation for a rectangular hyperbola.

The profiles of activity versus pH were fit to eq 1 to yield the two pK_a values.

$$v = \frac{V_{max}}{\frac{10^{-pH}}{10^{-pK_a1}} + \frac{10^{-pK_a2}}{10^{-pH}} + 1} \quad (1)$$

Kinetics of the Reductive Half-Reactions of the Glutamate Variants Using Stopped-Flow Spectrophotometry. The reductive half-reactions of the glutamate variants were studied by placing NADPH in anaerobic buffer in one syringe and oxidized enzyme in anaerobic buffer in the other syringe of the Hi-Tech SF-61 DX2 stopped-flow spectrophotometer at 25 °C. Enzymes (10 μM) were mixed with various concentrations of NADPH (10, 20, 30, 50, and 100 μM). Changes in the spectra during the reaction with NADPH were observed using a photodiode array detector, and absorbance changes at single wavelengths were monitored using a monochromator coupled to a photomultiplier detector. The dead time of the stopped-flow instrument is 1.5 ms, and the first spectrum was recorded starting 1.5 ms after the stop of flow. The apparent rate constants were derived from single-wavelength data with KinetAsyst (version 3.16) from Hi-Tech.

RESULTS AND DISCUSSION

Activity of the Glutamate Variants. The alignment of the protein sequences of TrxR from different species shows that two adjacent glutamate residues (Glu-469′ and Glu-470′) could potentially be involved in the catalysis of the interchange step (Figure S1 of the Supporting Information). Therefore, E469′A and E470′A DmTrxR were cloned and expressed. E469′A DmTrxR had 28% of the wild-type activity, whereas E470′A DmTrxR retained 70% of the wild-type activity (data not shown), indicating that Glu-469′ is more important to the catalysis than Glu-470′ is. The X-ray structure of DmTrxR shows that Glu-469′ is closer to His-464′ in the triad with Cys-57, consistent with this conclusion (*9*). To test the proposed idea that Glu-469′ makes His-464′ a better catalyst, it was of interest to study the effect of pH on the putative enhancement, utilizing both polar and apolar replacement residues for Glu-469′. Therefore, the effects of pH on the biochemical properties of E469′A and E469′Q DmTrxRs, including steady-state kinetics and the characteristics of the reductive half-reaction, were studied.

In the study of Benen et al., the activities of E455′D and E455′Q varants of lipoamide dehydrogenase from *Azotobacter vinelandii* retained only 1.6 and 1.2% of the wild-type activity, respectively, in the steady-state assays using an NAD^+ analogue as the electron acceptor (dihydrolipoamide to 3-acetylpyridine adenine dinucleotide, i.e., the physiological direction) (*24*). However, the histidine variants had even less than one percent of the wild-type activity, indicating that Glu was less important than His in the overall catalysis, as is the case with DmTrxR reported here. McMillan et al. showed that E514′A TrxR from *P. falciparum* (PfTrxR) had 7.5% of the wild-type activity, while the His-509′ variant had only 0.45% of the wild-type activity (*13*), again indicating that Glu was less important than His. E469′A and E469′Q DmTrxRs have 28 and 35% of the wild-type enzyme activity, respectively, indicating that like other members of the family, this glutamate residue has a secondary role in acid−base catalysis.

Considering the rather minimal effect of these substitutions in DmTrxR, it is possible that in the glutamate variants, the neighboring Glu-470′ may provide the function of Glu-469′ in its absence, with only modest alteration of the protein structure. Therefore, the E469′A/E470′A DmTrxR double variant was cloned and expressed to test this hypothesis. The activity of this variant had 25% of the wild-type enzyme activity, again indicating that the role of Glu-470′ is secondary and that it does not function effectively as an alternate for Glu-469′.

Effect of pH on the Steady-State Kinetics of the Glutamate Variants. The V_{max} and K_m values for the DmTrx-2 substrate for E469′A, E469′Q, and E469′A/E470′A variants at different pH values were determined using a fixed concentration of NADPH (100 μM). As shown in Figure 2A, the pH profiles for V_{max} of these three glutamate variants were shifted to somewhat more acidic pH values compared to that of the wild-type enzyme. The two pK_a values derived from the pH profiles of V_{max} for E469′A, E469′Q, and E469′A/E470′A DmTrxRs are approximately the same (pK_a = 6.0 ± 0.1 and 8.7 ± 0.2). For the sake of comparison, the two pK_a values determined for the wild-type enzyme are 6.4 ± 0.1 and 9.3 ± 0.13 (*12*). In our previous study, the pK_a of 6.4 ± 0.1 for the wild-type enzyme in complex with DmTrx-2 was attributed to contributions from both Cys-57 and Cys-490′, the attacking nucleophiles in the dithiol−disulfide interchange steps (*12*). This pK_a did not change in H464′Q DmTrxR, although the activity of H464′Q DmTrxR was much lower than that of the wild-type enzyme, suggesting

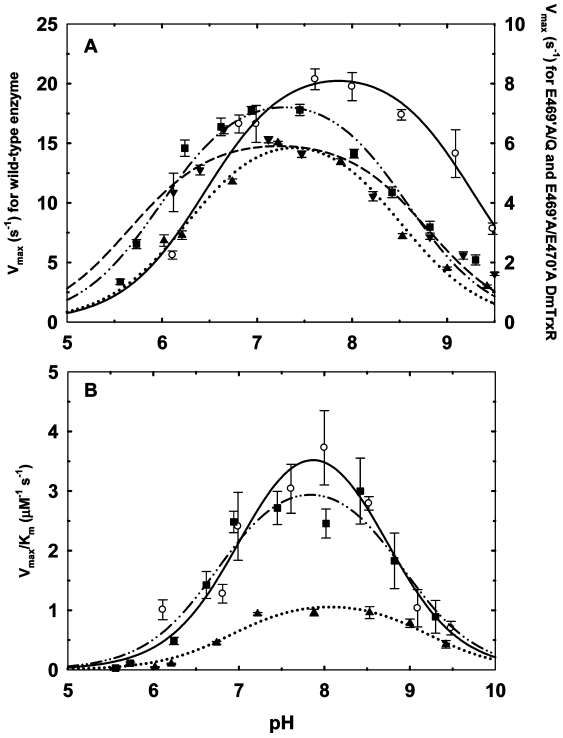

FIGURE 2: Steady-state kinetics of the wild-type enzyme and three glutamate variants at different pH values. (A) pH profiles of V_{max} for wild-type (—○—), E469′Q (—•·—■—•·—), E469′A (---▼---), and E469′A/E470′A (···▲···) DmTrxR. (B) pH profiles of V_{max}/K_m for wild-type (—○—), E469′Q (—•·—■—•·—), and E469′A/E470′A (···▲···) DmTrxR. The pH profile of V_{max}/K_m of E469′A DmTrxR is not shown here because the profiles of two glutamate variants are very similar. The K_m and V_{max} values were derived from a graph of turnover number vs DmTrx-2 concentration fit to an equation for a rectangular hyperbola. The data were fit to eq 1 to calculate the pK_a values.

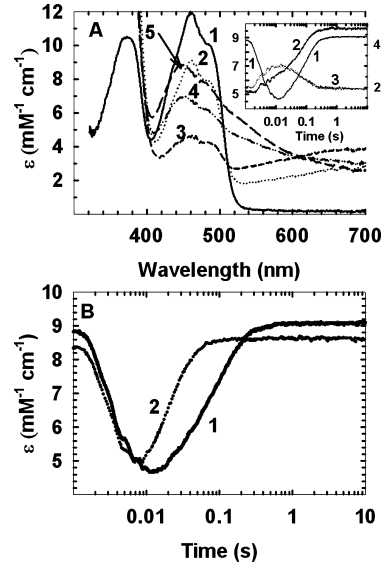

FIGURE 3: Spectra and kinetics observed in the reductive half-reactions of E469′A DmTrxR. Reduction was carried out at pH 7 and 25 °C under anaerobic conditions. (A) Reduction of DmTrxR (10 μM) with 10 equiv of NADPH: spectrum 1, oxidized enzyme; and spectra 2−5, 3, 10, 100, and 600 ms, respectively. The inset shows kinetic traces: curve 1, left *y*-axis, 450 nm; curve 2, right *y*-axis, 540 nm; and curve 3, right *y*-axis, 670 nm. (B) Kinetic traces at 450 nm and pH 7 (trace 1) and pH 9 (trace 2).

that the formation of thiolate anion in the variant is feasible but very inefficient. In the study presented here, the apparent pK_a of 6.0 ± 0.1 for V_{max}, contributed by Cys-57 and Cys-490′, is quite similar to that of the wild-type enzyme and is consistent with our previous assignment of this macroscopic pK_a value to Cys-57 and Cys-490′. The pK_a of 9.3 ± 0.13 assigned to His-464′ in our previous work changed to 8.7 ± 0.2 in the glutamate variants. This indicates that the basicity of His-464′ decreases in the absence of the negatively charged Glu-469′.

The two apparent pK_a values derived from the pH profiles of V_{max}/K_m of the three glutamate variants are 6.8 ± 0.15 and 9.0 ± 0.2 (Figure 2B) and virtually identical with those of the wild-type enzyme (*12*). The pK_a values derived from the pH profile of V_{max}/K_m are the macroscopic pK_a values of the free enzyme and substrate. We propose that the pK_a of 6.8 ± 0.15 is contributed by the nascent thiols on Cys-57 and Cys-490′. The pK_a of 9.0 ± 0.2 was initially assigned to His-464′. This work indicates that the assignment should be to the His-464′-Glu-469′ dyad. Figure 2B also shows that the double mutant E469′A/E470′A DmTrxR has a lower catalytic efficiency than wild-type and E469′Q DmTrxRs.

Effect of pH on the Reductive Half-Reaction of E469′Q and E469′A DmTrxR. Our previous results indicated that mutation of His-464′ inhibited the rate of flavin reduction by only 3.8-fold compared to that of the wild-type enzyme at pH 7 (formation of EH_2^A in Scheme 1); in contrast, the rates of disulfide reduction and subsequent interchange were inhibited profoundly, 120-fold (EH_2^B to EH_2^C and EH_2^D) (*12*). The reductive half-reactions of E469′Q and E469′A DmTrxR were studied here to determine whether the proposed function of Glu-469′ is to make His-464′ a stronger base for its interaction with Cys-57, a part of the reductive half-reaction. In addition, because the formation of thiolate anion is pH-dependent, we also compared the effect of pH on the reductive half-reactions of these two glutamate variants. Figures 3A and 4A show the spectra observed during the reductive half-reactions of E469′A and E469′Q DmTrxRs, respectively. Three apparent phases were identified from the kinetic traces (Figures 3A and 4A, insets). The first phase occurred from the dead time (1.5 ms) to ~10 ms, the second phase from ~10 to ~100 ms, and the third phase from ~100 to ~600 ms. In the first phase, the absorbance at 450 nm decreased and that at 670 nm increased, representing reduction of flavin and the formation of the $FADH^-$−$NADP^+$ CTC, respectively. These steps are associated with reduction of E_{ox} to EH_2^A (Scheme 1). In the second phase, the absorbance at 450 and 540 nm both increased, showing partial reoxidation of the flavin and formation of the thiolate−FAD CTC, respectively. Thus, this phase represents the reaction from EH_2^A to EH_2^B (Scheme 1). In the third phase (the slowest one), the absorbance at 450 and 540 nm continued to increase. This phase may not be due to a single step but could reflect the dithiol−disulfide interchange reaction between the N-terminal dithiol and the C-terminal disulfide (EH_2^B to EH_2^D), and the further reduction of EH_2 with the second molecule of NADPH to EH_4. The data of the wild-type enzyme in Figure 4A in Huang et al. (*12*) show a similar pattern but reflect the fact that the reactions are faster (see below).

The rates of the first phase of the reaction of NADPH with the glutamate variants were somewhat slower than those of the wild-type enzyme (1.2−1.9-fold) (Table 1), showing that

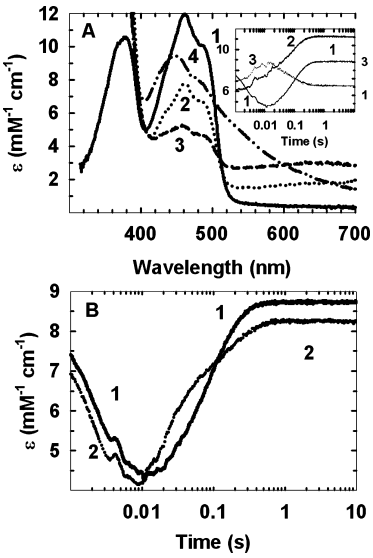

FIGURE 4: Spectra and kinetics observed in the reductive half-reactions of E469′Q DmTrxR. Reduction was carried out at pH 7 and 25 °C under anaerobic conditions. (A) Reduction of DmTrxR (10 μM) with 10 equiv of NADPH: spectrum 1, oxidized enzyme; and spectra 2−4, 1, 10, and 600 ms, respectively. The inset shows kinetic traces: curve 1, left *y*-axis, 450 nm; curve 2, right *y*-axis, 540 nm; and curve 3, right *y*-axis, 670 nm. (B) Kinetic traces at 450 nm and pH 7 (trace 1) and pH 9 (trace 2).

Table 1: Apparent Rate Constants Measured during the Reductive Half-Reactions of Wild-Type, E469′Q, and E469′A DmTrxR, at Different pH Values and 25 °C

enzyme[a]	pH	$K_{d,app}$(NADPH) (μM)[b]	$k_{1,app,max}$ (s^{-1})	$k_{2,app}$ (s^{-1})	$k_{3,app}$ (s^{-1})
wild type[c]	7	13 ± 4	629 ± 56	237 ± 37	47.4 ± 9.4
wild type[c]	8	8 ± 5	562 ± 83	187 ± 12	38 ± 16
wild type[c]	9	9 ± 2.8	488 ± 36	170 ± 23	16.4 ± 3.5
E469′A	7	21.5 ± 4.2	432 ± 30	14.2 ± 2.2	8 ± 1.4
E469′A	8	25 ± 3.6	465 ± 25	29 ± 2.0	9.4 ± 3.4
E469′A	9	17 ± 5.5	363 ± 38	69 ± 2.7	26.2 ± 8.2
E469′Q	7	15 ± 2.4	352 ± 17	13.4 ± 1.8	8 ± 1.4
E469′Q	8	20.2 ± 3	370 ± 19	36.6 ± 5.4	10.4 ± 1.4
E469′Q	9	15 ± 6.8	258 ± 7	78.2 ± 6.7	7.1 ± 0.5

[a] The concentration of enzyme was 10 μM. [b] The $K_{d,app}$(NADPH) values were determined from $k_{1,app}$ and different concentrations of NADPH using an equation for a rectangular hyperbola. $k_{1,app}$ reflects the reduction of the flavin. [c] The data have been published in our previous paper (*12*).

the transfer of hydride ion from NADPH to FAD was only slightly impaired in the glutamate variants. The second and third phases were much slower than those of the wild-type enzyme at pH 7 (17−18-fold) (Table 1), indicating that electron transfer from $FADH^-$ to the N-terminal redox-active disulfide and the subsequent dithiol−disulfide interchange reactions were significantly affected by the replacement of Glu-469′, as expected.

The rate of the second phase (EH_2^A to EH_2^B) of both glutamate variants increased at higher pH values, in contrast to that of the wild-type enzyme; the behavior of wild-type DmTrxR will be discussed below. Because the formation of thiolate anion on Cys-62, the product of this reaction, is favored at higher pH values, the rate of this phase in the variants is expected to increase as the pH is increased, and it does.

The effect of pH on the third rate constant (EH_2^B to EH_2^D) for these two glutamate variants is different. The rates observed in the third phase with E469′A DmTrxR were pH-dependent (Table 1), with the rate increasing at higher pH values. As discussed previously, this step is ascribed in part to the dithiol−disulfide interchange reaction between the N-terminal nascent dithiol pair and the C-terminal redox-active disulfide. The deprotonation of Cys-57, which is essential for the interchange reaction, will be enhanced at higher pH values as observed for E469′A DmTrxR. In contrast, the rate of the third phase of the reductive half-reaction in E469′Q DmTrxR was independent of pH (Table 1). In this variant, the active site is more polar than that in E469′A DmTrxR. It should be recalled that the flavin in this enzyme family is buried in the protein because the reduction of flavin by pyridine nucleotide and its reoxidation by disulfide require apolar conditions. However, His-464′ may still catalyze deprotonation of the thiol of Cys-57 and stabilize the resulting thiolate anion in E469′Q DmTrxR, because the glutamine residue may still form a hydrogen bond with His-464′, unlike the alanine residue. A quote from a recent paper from the Brocklehurst group shows that this is not a simple matter. "The nature of the kinetic consequences of electrostatic effects initiated by ionizations various distances from and with different orientations with respect to the catalytic site remains one of the least well understood aspects of enzyme active center chemistry, and there is considerable evidence that electrostatic effects are a major factor in determining the behavior of cysteine proteinases" (*28*). These workers present evidence indicating that the polarity of the milieu of the Cys-25-His-159 dyad in papain is affected primarily by Trp-177. However, earlier work from the same laboratory had indicated, just as convincingly, that Glu-50 was the principal affecter of dyad polarity, and the nearest carboxylate, that of Asp-158, had less influence (*29*).

Our previous study showed that the rate of the third phase with the wild-type enzyme decreased as the pH increased, as shown in Table 1. Although the formation of thiolate anion is favored at high pH, the formation of imidazolium on His-464′ is less favorable at higher pH values. This confirmed other data suggesting that the primary function of His-464′ is to stabilize the thiolate anion on Cys-57 via ion pair formation, with the promotion of thiolate formation being the less important function (*12*). Formation of a hydrogen bond between ND1 of the histidine residue and OE1 of the glutamine residue in E469′Q DmTrxR, similar to that which occurs in the wild-type enzyme with Glu-469′, might facilitate a productive orientation of His-464′ toward Cys-57, even if it were not ideal. The interaction of two linked factors may result in this phase being independent of pH. First, the thiolate anion on Cys-57 would be less stabilized for attack on Cys-490′ by the imidazolium of His-464′ in E469′Q DmTrxR than in the wild-type enzyme. Second, deprotonation of Cys-57 in E469′Q DmTrxR would still be affected by pH.

The kinetics of the reductive half-reaction of E469′A and E469′Q DmTrxRs at pH 7 are compared with those at pH 9 in Figures 3B and 4B, respectively. The biphasic nature of the increase in absorbance at 450 nm was more apparent at pH 9 than at pH 7 with E469′Q DmTrxR. This may reflect two enzyme populations whose relative concentrations depend on the charge state of His-464′.

Benen et al. showed that the spectra of the reduced glutamate variants, E455′D and E455′Q, of lipoamide dehydrogenase have high absorbance at 530 nm, contributed

by the thiolate−FAD CTC (*25*). McMillan et al. showed that in E514′A PfTrxR, the thiolate−FAD CTC is also enhanced (*13*). The thiolate−FAD CTC contributing to absorbance at 540 nm was also enhanced in both glutamate variants of DmTrxR (Figure 3, spectrum 5, and Figure 4, spectrum 4). It is highly likely that enhancement of the CTC results from subtle changes in the polarity of the active site. Our data show that the absorbance at 670 nm contributed by the $FADH^-$−$NADP^+$ CTC was higher in E469′Q and E469′A DmTrxRs than in the wild-type enzyme (Figures 3 and 4, spectrum 3). The higher CTC is partially due to electron transfer to the proximal disulfide being slower in these variants so that more of the $FADH^-$−$NADP^+$ CTC builds up, and possibly also to tighter binding of $NADP^+$.

The K_d values of NADPH were calculated using plots of the apparent first-order rate constants versus NADPH concentration. As shown in Table 1, the binding of NADPH to the glutamate variants was slightly less tight than to the wild-type enzyme. Like that in the wild-type enzyme, the effect of pH on the dissociation constant of NADPH for both glutamate variants was not significant. The second and third rate constants were nearly independent of the concentration of NADPH.

CONCLUDING STATEMENTS

Malaria is the cause of a serious public health issue globally; 500 million cases are reported anually, and 2.5 million people die of this disease annually (*30*). The malarial parasites of the genus *Plasmodium* and its vector, *A. gambiae*, have extremely high demands for the Trx system because of high rates of production of reactive oxygen species. Structural and mechanistic differences among TrxRs from humans and from *A. gambiae* and *P. falciparum* have been observed (*9, 12, 13, 31*). Specifically, in this study, we have discovered that Glu-469′ in DmTrxR is less sensitive to the effects of mutation than the analogous Glu-514′ from *P. falciparum* is. We hope that the recognition of these differences may aid in the development of differential inhibitors more specific for TrxR from the parasites. Thus, similar studies should be extended to the human enzyme.

The thiolate−imidazolium−carboxlate catalytic triad is conserved in the enzymes of the family of pyridine nucleotide-disulfide oxidoreductases, and the glutamate-histidine dyad has been shown to act as an acid−base catalyst (*13*−*15, 22, 24, 25*). Indeed, the function of the histidine residue in TrxRs has been studied, and this amino acid residue is crucial to catalysis (*12, 13*). However, the role of the glutamate residue in the thioredoxin reductase family had not been fully addressed (*13*−*15*). This led us to explore the role of the glutamate residue in the catalysis of DmTrxR.

Examination of the sequence alignments shows that only TrxRs from dipteran insects have two adjacent glutamate residues (Glu-469′ and Glu-470′ in DmTrxR), both of which could potentially be involved in the catalysis (Figure S1 of the Supporting Information). Our data showed that Glu-469′ is more important than Glu-470′ in the catalysis of DmTrxR. It was of interest to study the biochemical properties of the glutamate variants utilizing both polar and apolar replacement residues for Glu-469′, the homologous glutamate.

The two glutamate variants of Glu-469′ lost only ∼70% of their activity, suggesting that this glutamate residue is important but not critical to the catalysis of DmTrxR. The short distance between His-464′ and Glu-469′ shows that a hydrogen bond exists between these two amino acid residues; formation of a LBHB is possible during the catalysis of DmTrxR if the pK_a values of these two residues match, which has been observed with the serine proteases (*16, 32*). The V_{max} versus pH profile shows that the mutation of Glu-469′ causes a decrease in the basicity of His-464′ in a complex of the enzyme with DmTrx-2.

The rates of the three phases of the reductive half-reaction were inhibited in both glutamate variants. The second phase, associated with reduction of the N-terminal disulfide by $FADH^-$, and the third phase, associated in part with dithiol−disulfide interchange, were significantly slower in both glutamate variants. The inhibitory effects due to the mutation of Glu-469′ on the second and third phases were smaller at higher pH values in E469′A DmTrxR, as one would expect because the formation of thiolate anion is favored at higher pH values.

The data from this study strongly indicate that the function of Glu-469′ is to enhance the basicity of His-464′, perhaps by facilitating its orientation toward Cys-57.

ACKNOWLEDGMENT

We are grateful to Dr. Stephan Gromer (University of Heidelberg) and Prof. Katja Becker (University of Giessen, Giessen, Germany) for supplying the vector used in the site-directed mutagenesis and Dr. Michael Tarasev for his help in the design of primers for site-directed mutagenesis.

SUPPORTING INFORMATION AVAILABLE

Primers used to clone E469′A, E469′Q, E470′A, and E469′A/E470′A DmTrxR (Table S1) and alignment of sequences of TrxRs from different species (Figure S1). This material is available free of charge via the Internet at http://pubs.acs.org.

REFERENCES

1. Williams, C. H. J. (1992) *Chemistry and Biochemistry of Flavoenzyme*, Vol. 3, CRC Press, Boca Raton, FL.
2. Williams, C. H., Arscott, L. D., Muller, S., Lennon, B. W., Ludwig, M. L., Wang, P. F., Veine, D. M., Becker, K., and Schirmer, R. H. (2000) Thioredoxin reductase two modes of catalysis have evolved. *Eur. J. Biochem. 267*, 6110–6117.
3. Moore, E. C., Reichard, P., and Thelander, L. (1964) Enzymatic Synthesis of Deoxyribonucleotides. V. Purification and Properties of Thioredoxin Reductase from *Escherichia Coli* B. *J. Biol. Chem. 239*, 3445–3452.
4. Benhar, M., Forrester, M. T., Hess, D. T., and Stamler, J. S. (2008) Regulated protein denitrosylation by cytosolic and mitochondrial thioredoxins. *Science 320*, 1050–1054.
5. Holmgren, A. (2008) Biochemistry. SNO removal. *Science 320*, 1019–1020.
6. Kanzok, S. M., Fechner, A., Bauer, H., Ulschmid, J. K., Muller, H. M., Botella-Munoz, J., Schneuwly, S., Schirmer, R., and Becker, K. (2001) Substitution of the thioredoxin system for glutathione reductase in *Drosophila melanogaster*. *Science 291*, 643–646.
7. Bauer, H., Gromer, S., Urbani, A., Schnolzer, M., Schirmer, R. H., and Muller, H. M. (2003) Thioredoxin reductase from the malaria mosquito *Anopheles gambiae*. *Eur. J. Biochem. 270*, 4272–4281.
8. Bauer, H., Massey, V., Arscott, L. D., Schirmer, R. H., Ballou, D. P., and Williams, C. H., Jr. (2003) The mechanism of high Mr thioredoxin reductase from *Drosophila melanogaster*. *J. Biol. Chem. 278*, 33020–33028.
9. Eckenroth, B. E., Rould, M. A., Hondal, R. J., and Everse, S. J. (2007) Structural and biochemical studies reveal differences in the

catalytic mechanisms of mammalian and *Drosophila melanogaster* thioredoxin reductases. *Biochemistry 46*, 4694–4705.
10. Luthman, M., and Holmgren, A. (1982) Rat liver thioredoxin and thioredoxin reductase: Purification and characterization. *Biochemistry 21*, 6628–6633.
11. Gromer, S., Johansson, L., Bauer, H., Arscott, L. D., Rauch, S., Ballou, D. P., Williams, C. H., Jr., Schirmer, R. H., and Arner, E. S. (2003) Active sites of thioredoxin reductases: Why selenoproteins? *Proc. Natl. Acad. Sci. U.S.A. 100*, 12618–12623.
12. Huang, H. H., Arscott, L. D., Ballou, D. P., and Williams, C. H., Jr. (2008) Acid-Base Catalysis in the Mechanism of Thioredoxin Reductase from *Drosophila melanogaster*. *Biochemistry 47*, 1721–1731.
13. McMillan, P. J., Arscott, L. D., Ballou, D. P., Becker, K., Williams, C. H., Jr., and Muller, S. (2006) Identification of acid-base catalytic residues of high-Mr thioredoxin reductase from *Plasmodium falciparum*. *J. Biol. Chem. 281*, 32967–32977.
14. Brandt, W., and Wessjohann, L. A. (2005) The functional role of selenocysteine (Sec) in the catalysis mechanism of large thioredoxin reductases: Proposition of a swapping catalytic triad including a Sec-His-Glu state. *ChemBioChem 6*, 386–394.
15. Gromer, S., Wessjohann, L. A., Eubel, J., and Brandt, W. (2006) Mutational studies confirm the catalytic triad in the human selenoenzyme thioredoxin reductase predicted by molecular modeling. *ChemBioChem 7*, 1649–1652.
16. Cleland, W. W., Frey, P. A., and Gerlt, J. A. (1998) The low barrier hydrogen bond in enzymatic catalysis. *J. Biol. Chem. 273*, 25529–25532.
17. Qian, J., Khandogin, J., West, A. H., and Cook, P. F. (2008) Evidence for a catalytic dyad in the active site of homocitrate synthase from *Saccharomyces cerevisiae*. *Biochemistry 47*, 6851–6858.
18. Craik, C. S., Roczniak, S., Largman, C., and Rutter, W. J. (1987) The catalytic role of the active site aspartic acid in serine proteases. *Science 237*, 909–913.
19. Ishida, T., and Kato, S. (2004) Role of Asp102 in the catalytic relay system of serine proteases: A theoretical study. *J. Am. Chem. Soc. 126*, 7111–7118.
20. Sprang, S., Standing, T., Fletterick, R. J., Stroud, R. M., Finer-Moore, J., Xuong, N. H., Hamlin, R., Rutter, W. J., and Craik, C. S. (1987) The three-dimensional structure of Asn102 mutant of trypsin: Role of Asp102 in serine protease catalysis. *Science 237*, 905–909.
21. Frey, P. A., Whitt, S. A., and Tobin, J. B. (1994) A low-barrier hydrogen bond in the catalytic triad of serine proteases. *Science 264*, 1927–1930.
22. Pai, E. F., and Schulz, G. E. (1983) The catalytic mechanism of glutathione reductase as derived from X-ray diffraction analyses of reaction intermediates. *J. Biol. Chem. 258*, 1752–1757.
23. Karplus, P. A., and Schulz, G. E. (1987) Refined structure of glutathione reductase at 1.54 Å resolution. *J. Mol. Biol. 195*, 701–729.
24. Benen, J., van Berkel, W., Dieteren, N., Arscott, D., Williams, C., Jr., Veeger, C., and de Kok, A. (1992) Lipoamide dehydrogenase from *Azotobacter vinelandii*: Site-directed mutagenesis of the His450-Glu455 diad. Kinetics of wild-type and mutated enzymes. *Eur. J. Biochem. 207*, 487–497.
25. Benen, J., van Berkel, W., Zak, Z., Visser, T., Veeger, C., and de Kok, A. (1991) Lipoamide dehydrogenase from *Azotobacter vinelandii*: Site-directed mutagenesis of the His450-Glu455 diad. Spectral properties of wild type and mutated enzymes. *Eur. J. Biochem. 202*, 863–872.
26. Cheng, Z., Arscott, L. D., Ballou, D. P., and Williams, C. H., Jr. (2007) The relationship of the redox potentials of thioredoxin and thioredoxin reductase from *Drosophila melanogaster* to the enzymatic mechanism: Reduced thioredoxin is the reductant of glutathione in *Drosophila*. *Biochemistry 46*, 7875–7885.
27. Kooter, I. M., Steiner, R. A., Dijkstra, B. W., van Noort, P. I., Egmond, M. R., and Huber, M. (2002) EPR characterization of the mononuclear Cu-containing *Aspergillus japonicus* quercetin 2,3-dioxygenase reveals dramatic changes upon anaerobic binding of substrates. *Eur. J. Biochem. 269*, 2971–2979.
28. Gul, S., Hussain, S., Thomas, M. P., Resmini, M., Verma, C. S., Thomas, E. W., and Brocklehurst, K. (2008) Generation of nucleophilic character in the Cys25/His159 ion pair of papain involves Trp177 but not Asp158. *Biochemistry 47*, 2025–2035.
29. Pinitglang, S., Watts, A. B., Patel, M., Reid, J. D., Noble, M. A., Gul, S., Bokth, A., Naeem, A., Patel, H., Thomas, E. W., Sreedharan, S. K., Verma, C., and Brocklehurst, K. (1997) A classical enzyme active center motif lacks catalytic competence until modulated electrostatically. *Biochemistry 36*, 9968–9982.
30. Linares, G. E., and Rodriguez, J. B. (2007) Current status and progresses made in malaria chemotherapy. *Curr. Med. Chem. 14*, 289–314.
31. Fritz-Wolf, K., Urig, S., and Becker, K. (2007) The structure of human thioredoxin reductase 1 provides insights into C-terminal rearrangements during catalysis. *J. Mol. Biol. 370*, 116–127.
32. Cleland, W. W., and Kreevoy, M. M. (1994) Low-barrier hydrogen bonds and enzymic catalysis. *Science 264*, 1887–1890.
33. Sandalova, T., Zhong, L., Lindqvist, Y., Holmgren, A., and Schneider, G. (2001) Three-dimensional structure of a mammalian thioredoxin reductase: Implications for mechanism and evolution of a selenocysteine-dependent enzyme. *Proc. Natl. Acad. Sci. U.S.A. 98*, 9533–9538.

BI801449H